Author/s:
Zhang, B;Yang, H;Warner, T;Mulvaney, P;Rosengarten, G;Wong, WWH;Ghiggino, KP

Title:
A luminescent solar concentrator ray tracing simulator with a graphical user interface: Features and applications

Date:
2020-07-01

Citation:
Zhang, B., Yang, H., Warner, T., Mulvaney, P., Rosengarten, G., Wong, W. W. H. & Ghiggino, K. P. (2020). A luminescent solar concentrator ray tracing simulator with a graphical user interface: Features and applications. Methods and Applications in Fluorescence, 8 (3), https://doi.org/10.1088/2050-6120/ab993d.

Persistent Link:
https://hdl.handle.net/11343/337141

Methods and Applications in Fluorescence

A luminescent solar concentrator ray tracing simulator with a graphical user interface: Features and applications

To cite this article before publication: Bolong Zhang *et al* 2020 *Methods Appl. Fluoresc.* in press https://doi.org/10.1088/2050-6120/ab993d

A luminescent solar concentrator ray tracing simulator with a graphical user interface: Features and applications

Bolong Zhang,[1,2#] Hanbo Yang,[1#] Timothy Warner,[1,3] Paul Mulvaney,[1] Gary Rosengarten,[3] Wallace W. H. Wong[1,2] and Kenneth P. Ghiggino[1*]

[1]School of Chemistry and ARC Centre of Excellence in Exciton Science, University of Melbourne, Victoria 3010, Australia

[2]Bio21 Institute, University of Melbourne, 30 Flemington Road, Victoria 3010, Australia

[3]School of Mechanical and Automotive Engineering and ARC Centre of Excellence in Exciton Science, RMIT University, Melbourne 3001, Australia

#co-first authors

* Author for correspondence

Abstract:

A Monte-Carlo ray tracing simulator with a graphical user interface (MCRTS-GUI) has been developed to provide a quantitative description, performance evaluation and photon loss analysis of luminescent solar concentrators (LSCs). The algorithm is applied to several practical LSC device structures including multiple dyes in the same waveguiding layer, and structures where a dye layer is sandwiched between clear substrates. The effect of the host matrix absorption and the influence of the neighboring layers are investigated. Validations demonstrate that the MCRTS-GUI developed provides a reliable and accurate description of LSC performance. Code for the mixed-dye single layer configuration is converted into a ray-tracing package with a user-friendly interface and is made available as open source software.

Introduction

Luminescent solar concentrators (LSCs) have been proposed as efficient, low-cost devices for use in integrated photovoltaics (PV).[1-2] A typical LSC consists of a planar waveguide made of either glass or plastic (Figure 1a).[3] The waveguide is coated or embedded with fluorescent dyes that absorb a portion of the solar spectrum and emit luminescence at a lower energy.[3] A large fraction of the emitted light is preferentially transported to the edges of the LSC, due to total internal reflection, where PV cells are attached. There are two major types of LSCs depending on the device structure, namely bulk-doped and thin-film LSCs (Figure 1b).[4] The bulk-doped LSC refers to a device with the dyes embedded in a homogenous waveguide matrix, while a thin-film LSC consists of a thin dye-layer deposited on the surface of a clear waveguiding matrix.

The performance of a LSC is theoretically limited by a number of loss mechanisms, namely, the transmittance loss, the escape-cone loss, and the non-unity photoluminescence quantum yield (PLQY) of the fluorophore system (Figure 1a).[5-6] The transmittance loss results from the limited range of incident light that is matched by the dye's absorption range. The escape-cone loss refers to the photons that are not trapped in the waveguide by total-internal reflection and are lost through the top and bottom faces of the device. The PLQY of the fluorophore system determines the fraction of absorbed photons that are emitted by the dye molecule.[7] Re-absorption of emitted photons leads to an increase in both the escape-cone losses and emission losses. The amount of re-absorption of emitted photons is determined by the

spectral overlap of the emission and absorption of the fluorophore system, so a large Stokes shift is desirable for efficient LSC device performance. In practice, the surface roughness and the absorbance of the waveguide substrate itself may also significantly influence the LSC performance.

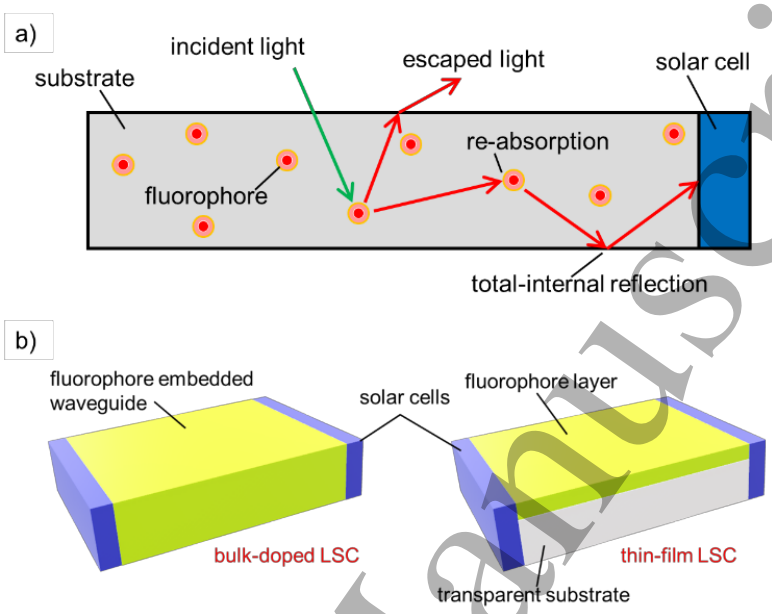

Figure 1 a) optical processes within a LSC and b) the structures of a bulk-doped LSC and a thin-film LSC.

The photophysical properties of the fluorophore, the waveguide material, the size and shape of the LSC and the incident light source are all determining factors in the waveguiding process. These parameters are interdependent and are not intuitive. Modelling provides guidance to optimize the performance of LSCs. Two approaches commonly adopted are the thermodynamic model and ray-tracing model.[8-9] The thermodynamic model requires fewer inputs but is limited to LSCs with a single type of participating species. The Monte Carlo ray-trace simulation (MCRTS) is more versatile in allowing multiple dopants and device geometries. MCRTS is a semi-empirical modelling method which relies on experimental inputs to predict the trajectories of photons (rays) inside a waveguide, and the efficiency of a LSC.[10] The method integrates over the incident spectral photon flux and records the progress of a light ray and its interaction with the matrix components using laws of reflection and refraction and the photoluminescence properties of the dyes. To date, most of the MCRTS packages reported simulate the trajectories of light in complex models or render realistic images that are either computationally demanding or without a graphical user interface (GUI).[11-12] We have developed and evaluated a MCRTS-GUI that focusses on the simulation of planar LSCs to provide outputs with a relative standard error of less than 1 %.

In this paper, we describe a user friendly MCRTS-GUI that allows for simulations of a rectangular waveguide with up to two participating fluorophores and up to two additional clear substrate layers. Both the size and refractive index (n) of the waveguide and the incident light source can be customized in the MCRTS. We provide user guidelines along with a walk-through of the graphical user interface. A theoretical validation of the model is presented, and a comprehensive analysis of a dual-fluorophore system is provided using the luminescent dyes Coumarin 6 and Lumogen F Red 305 (LR305), which have been widely used in LSCs by both ourselves and others.[13-16] These dyes have high fluorescence quantum yields in polymer film environments (> 0.7) and are relatively photostable. They do, however, exhibit

significant re-absorption and are known to undergo self-quenching at high concentrations. These deficiencies for LSCs, and the ways that might be addressed, have been discussed by us previously.[14-15] Since the dyes chosen exhibit the range of photophysical behaviors that are often encountered in LSC studies, they provide useful examples for testing the performance of the simulation packages reported in this work. Of course, the program can be used for any dye system, and not limited to Coumarin 6 or LR305. A series of simulations are also described for a three-layer LSC structure to reveal the influence of n on both the dye-layer and the clear substrate layers.

Model Overview

The program assumes that the classical ray model of light holds, where light moves in a straight line unless it encounters a participating particle or an interface. A light ray can be reflected, absorbed or transmitted. Dye particles are assumed to be both monodisperse (i.e. not aggregates) and homogeneously distributed inside the host matrix. As shown in the flow chart in Figure 2a, the simulation considers and counts all of the theoretical losses of rays travelling in the dual-dye waveguide system.

The MCTRS-GUI relies on several experimental inputs to run statistical analyses of the LSC device. The photons generated at a normal incident angle to the top surface of the LSC comprise wavelengths of illumination specified by a given spectral profile. In a dual-dye system, the distance a ray travels before absorption or re-absorption (ray distance, Δl) is derived from the Beer-Lambert law (Eq. 1):

$$\ln \frac{I_0}{I} = \varepsilon(\lambda) c l \qquad \text{Eq. 1}$$

where the relationship between the incident intensity (I_0) and transmitted intensity (I) of a ray is described by its spectral molar absorption coefficient, $\varepsilon(\lambda)$ ($\mathrm{L.mol^{-1}.cm^{-1}}$), the concentration, c ($\mathrm{mol.\,L^{-1}}$) of dye in a film, with thickness, l (cm).

The distance a ray travels before re-absorption (ray distance, Δl) is related to the absorptivity (α) of the dye in a dual-dye system, represented by dye 1 and dye 2 (Eq. 2).

$$\Delta l = \frac{\ln \frac{1}{1-\alpha}}{\varepsilon(\lambda)_1 c_1 + \varepsilon(\lambda)_2 c_2} \qquad \text{Eq. 2}$$

where α is given as a random number between 0 and 1 ($0 < \alpha < 1$). Based on the ratio of the relative individual dye absorption probabilities, the dye that absorbs the photon is determined. The probability of the photon being emitted depends on the PLQY of the respective dye. The isotropically emitted photon is assigned a down converted wavelength weighted by the dye's emission spectrum.

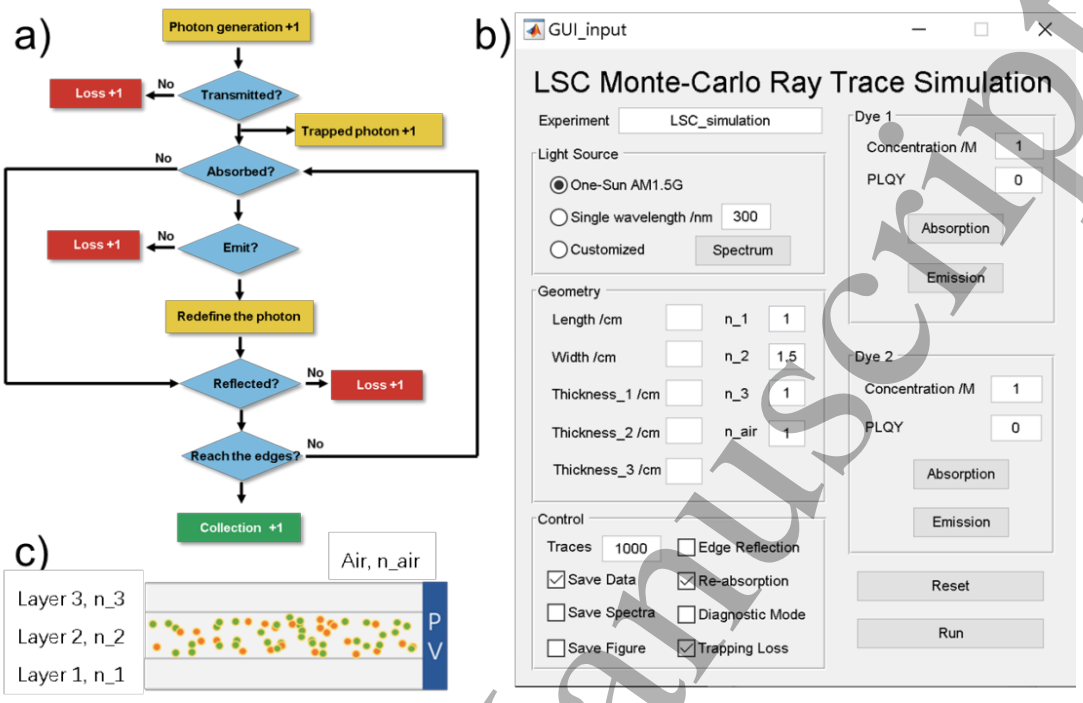

Figure 2 a) A flow chart illustrating the simulation cycle employed in the MCRTS-GUI, b) the window of the GUI and c) the virtual waveguide structure in the MCRTS-GUI. Layers 3 and 1 are clear substrates with no matrix absorption, and layer 2 is embedded with dyes.

Depending on the random path, a photon can be trapped by internal reflection from all faces of the LSC. If the solar cells are not optically coupled to the LSC, internal reflection will occur instead of collection by the solar cell. The user can specify that only internal reflection occurs from the top and bottom faces of the LSC; the solar cells and the LSC are optically coupled; and any photon reaching the edges is collected. The ray is trapped inside the film if the angle of incidence is smaller than the critical angle at the interface. The wavelength is recorded for any unabsorbed, trapped ray. If the ray's emitted wavelength overlaps its absorption wavelength, re-absorption events will occur. The MCRTS will record the outcome of photons in each simulation cycle and provide the probability distribution as an indication of LSC device performance.

Instructions for use of the MCRTS-GUI

MATLAB® 2016a or higher version is required to run the MCRTS-GUI. A compressed version of the MCRTS-GUI codes can be freely downloaded from http://blogs.unimelb.edu.au/uml/**lsc-matlab-code/**. Once downloaded, all the files should be uncompressed into one folder in the user's computer. The user needs to run the file **Monte_Carlo_Simulation.m** in MATLAB to activate the GUI (Figure 2b).

Experiment: the user can customize the experiment name for the simulation.

Light source panel: The user can choose the incident light source from AM1.5g, single-wavelength or a customized spectrum. When choosing the single-wavelength mode, the user is required to specify the wavelength. For using the customized spectrum mode, the user can provide the spectrum by clicking on the 'Spectrum' button.

Waveguide panel: The MCRTS-GUI allows the user to simulate a single junction rectangular waveguide system. The waveguide system should have one dye layer (Layer 2) and at most two clear substrate layers (Layer 1 and Layer 3) on the top and bottom of the dye layer respectively (Figure 2c). The user can customize the substrate materials of each layer by modifying their refractive index (n). Therefore, MCRTS-GUI can simulate both a thin-film LSC and a bulk-doped LSC.

Control panel: The user can customize the number of rays being simulated in one experiment, which further influences the accuracy of the simulation. The specified number of rays accounts for photons that are initially absorbed whereas transmitted photons are in addition to this number. The number of rays is set to 1000 by default, but a ray number of no less than 10,000 is recommended for higher accuracy.

Dye 1 and Dye 2: Dye properties including the concentration (M) and PLQY (0-1) are specified here as constants. Absorption and emission spectra are inputs with wavelengths to cover the range 300 to 800 nm. All absorbance values must be positive, and the longest absorption wavelength needs to be smaller than the longest emission wavelength.

Save Data: MCRTS-GUI will save the simulation results sequentially in the 'Result' folder under the filename 'output.txt' by default. The user can also read the result output in the Command Window in MATLAB. Additionally, a .csv file will be generated using the experiment name as a title which contains the results. When a simulation is completed, 'Simulation is now completed.' will be shown in the Command Window.

The MATLAB code outputs the following values:

- Collected photons from the edges of the waveguide. The flux gain (F), external quantum efficiency (EQE) and geometric gain (G) of a LSC which are related as follows.

$$F = EQE \times G \quad \text{Eq. 3}$$

- The EQE of a LSC defined as the ratio of number of photons collected at the edges (n_{edges}) to the number of incident photons (n_{incident}).

$$EQE = \frac{n_{\text{edges}}}{n_{\text{incident}}} \quad \text{Eq. 4}$$

- G is defined as the ratio of the incident area A_{incident} to the output edge area A_{edges}.

$$G = \frac{A_{\text{incident}}}{A_{\text{edges}}} \quad \text{Eq. 5}$$

- **Escape cone loss** is the fraction of emitted photons that are transmitted through the top and bottom faces.
- **Reabsorbed** is the number of reabsorbed photons.
- **OQE** is the ratio of photons collected over the absorbed photons.
- **Transmission fraction** is the fraction of light from the excitation source that is not being absorbed by the dyes.
- **Trapping efficiency** is the ratio of the number of photons collected at the edges to the total number of photons exiting from all the LSC surfaces.
- **Average ray distance** is the average distance a light ray will travel in the waveguide.

Save Spectra: The user can choose to save the simulated spectra to the 'Result' folder. The spectra include both the edge-collected photons and the surface-escaped photons. Saving the spectra will slightly increase the run time. A new simulation will overwrite the previous spectra, unless saved separately.

Save Figures: This option allows the user to graphically view the trajectories of the photons inside a LSC. A 2D side-view and a 3D view of the LSC will be displayed at the end of the simulation. 'Save Figures' will increase the simulation time significantly and thus this option is not recommended for ray numbers over 100,000.

Edge-reflection: By default, all the photons will be collected once they reach any edge of the waveguide, unless the user 'ticks' this box.

Re-absorption: The simulation will include re-absorption events by default, unless the user 'un-ticks' this box.

Diagnostic mode: This mode forces the incident light to the central position of the waveguide. The diagnostic mode can provide additional insights in some simulation experiments.

Trapping loss: When a photon is trapped in the waveguide for an excessive period, the code will stop the photon event to control the simulation time. The trapped photon will be considered lost via absorption by the waveguide substrate by default; alternatively, it is considered lost via the escape-cone if the box is 'un-ticked'.

Dye panel: MCRTS-GUI allows the user to simulate at most two independent dye systems in the waveguide. The user is required to input the dye concentration (M), PLQY (0 to 1), absorption coefficient ($\varepsilon(\lambda)$) spectrum and emission spectrum of each dye system. For simulating a single dye system the absorption coefficient spectrum of Dye 2 should be set to 0 at all wavelengths. The concentration of both dye systems should be > 0.

Reset: Restart the simulation and resets all variables to the default values.

Run: Run the experiment based on the input conditions. When the simulation is completed, the statement 'Simulation is now completed' will be shown in the Command Window in MATLAB.

Table 1 Error and run time for a set number of rays, assuming the absorbance of the LSC is 1. When the absorbance of the LSC is lower, the run time increases.

Number of rays	Stdev	%RSD[a]	Run time (s)[b]
100	0.0443	5.93	0.08
1,000	0.0145	1.96	0.27
10,000	0.0045	0.61	1.88
100,000	0.0014	0.18	17.80
1,000,000	0.0004	0.06	177.14

[a] Relative Standard Deviation

[b] The run time of MCRTS-GUI is calculated using a typical laboratory desktop computer (Dell 9th Gen Intel® Core™ i7 9700). The actual run time will depend on the performance of the computer used.

Simulations and discussion

A series of simulations were performed based on the MCRTS-GUI for validation and to provide examples of the code operation. The first simulation mimics the Beer-Lambert Law[17] and was used to validate the photon absorption process in MCRTS-GUI. For this case a single wavelength light source was used in the simulation and the n of the waveguide substrate was set to 1 to exclude the influence of surface reflectance. The number of rays was set to 10,000 at each wavelength with the dye PLQY = 0. The simulated absorbance at a single wavelength (λ = 523 nm) is plotted as a function of the waveguide thickness and the fluorophore concentration in Figure 3a and 3b respectively and shows excellent agreement with theoretical Beer-Lambert behaviour. As shown in Figure 3c, the simulated absorbance matches very well with the experimental absorbance for LR305 measured over the whole spectrum in a cuvette with a 1 cm light path. This simple validation demonstrates that the method used to generate large numbers of random photons and to simulate their absorption within the matrix is reliable and accurate.

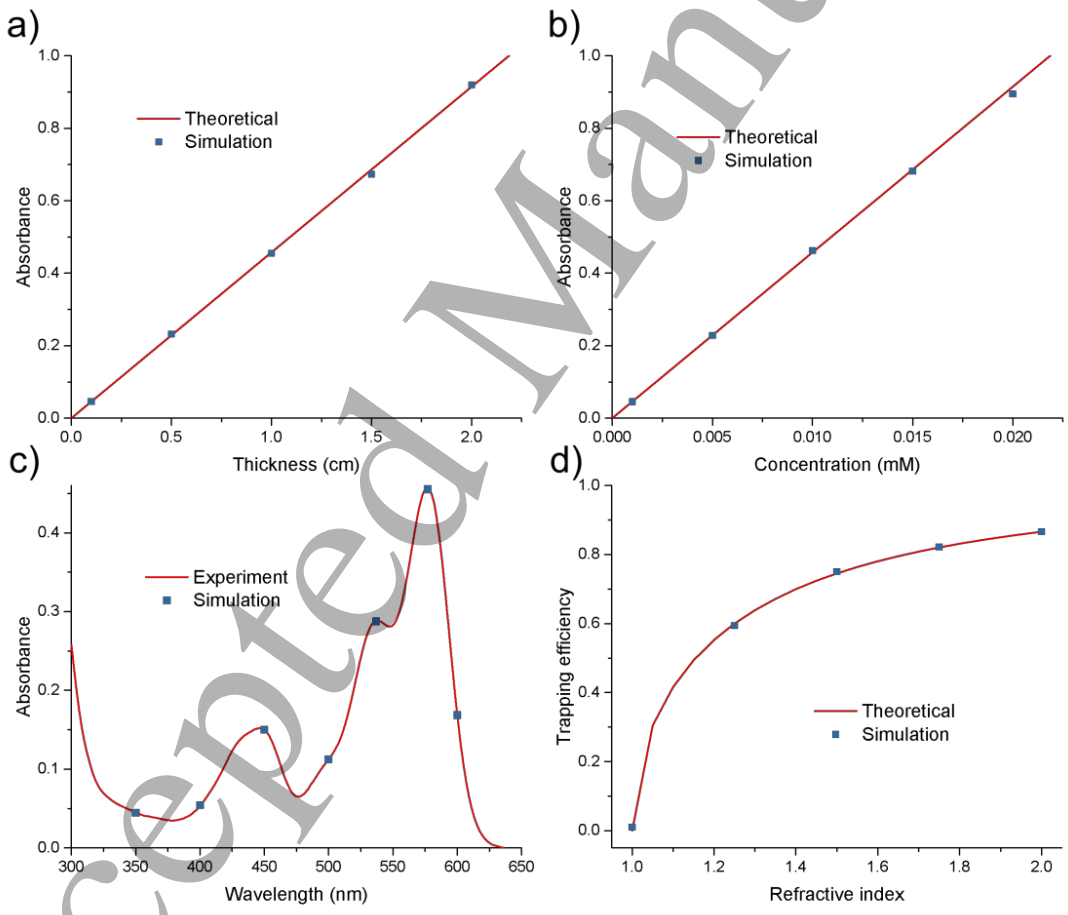

Figure 3. Comparison between theoretical and simulated absorbance (λ = 523 nm) of LR305 in a waveguide against a) the thickness and b) the concentration. c) Comparison between the experimental and the simulated absorbance spectra of LR305 (0.01 mM) in 1 cm light path. d) Comparison of the

theoretical and simulated trapping efficiency of LR305 in a waveguide (10 x 10 x 0.1 cm) against the n of the substrate materials. The number of rays is 10,000 for all data points (with RSD of 0.61%).

The ability of the MCRTS-GUI to account for Snell's Law[18] losses (top and bottom surface reflections) was also tested as a function of the matrix n. The fraction of the escape-cone loss (η_{escape}) is directly related to the n of the substrate material ($n_{\mathrm{substrate}}$) in the waveguide:

$$\eta_{\mathrm{escape}} = 1 - \eta_{\mathrm{trapping}} = 1 - \sqrt{1 - \left(\frac{n_{\mathrm{air}}}{n_{\mathrm{substrate}}}\right)^2} \quad \text{Eq. 6}$$

where η_{trapping} refers to the trapping efficiency of the waveguide and n_{air} is the n of air. When using glass or PMMA as the waveguide substrate material, where $n_{\mathrm{substrate}}$ is 1.5, the value of η_{escape} is 25.5%. However, the substrate materials of the waveguide can be replaced by materials such as quartz or plastic which have different refractive indices. The trapping efficiency of the waveguide is accurately replicated by the model which allows the users to customize the substrate materials of the waveguide by varying the n.

For the simulation, η_{escape} and η_{trapping} can be further defined as the fraction of the escaped and trapped photons per absorbed photons in the waveguide respectively. LR305 (0.0001 mM) was used as the fluorophore embedded in a bulk-LSC (10 x 10 x 0.1 cm) in the simulation. The PLQY of LR305 was set to 1 and the re-absorption mode was switched off to exclude external influences. Consequently, the value of η_{escape} and η_{trapping} are only dependent on the n of the waveguide. The theoretical $\eta_{trapping}$ was plotted against the n of the waveguide using Equation 1 and is shown in Figure 3d. The simulated η_{trapping} was very well matched with the theoretical η_{trapping}, indicating the MCRTS-GUI can precisely simulate the escape-cone loss process of LSCs.

Simulated results for the 2-dye system are shown in Figure 4 using the PLQY values determined for Coumarin 6 (0.78) and LR305 (0.98) in solid PMMA. As discussed earlier, Coumarin 6 and LR305 have been widely used in LSCs and their photophysics has been well characterised.[13-16] They do exhibit features that can be detrimental to LSC performance including fluorescence re-absorption. We can assume only radiative processes need be considered at the low concentrations considered here (i.e. no energy transfer takes place as fluorophore separation is much greater than the critical transfer distance). However, the LR305 dye can re-absorb its own luminescence and also absorb the photons emitted from Coumarin 6 as indicated from the spectra shown in Figure 4a. This situation provides a typical example of issues that can be encountered a 2-dye system that might affect LSC performance. As shown in Figure 4b, increasing the concentration of LR305 and coumarin 6 had a disproportionate effect on the flux gain of the system (under AM1.5g). Adding more LR305 is more advantageous than increasing the absorption levels of Coumarin 6. The fates of absorbed photons were identified using the MCRTS-GUI (Figure 4c) and it was found that by increasing the concentration ratio of LR305:Coumarin 6, the fraction of photons lost because of non-unity PLQY decreased while the escape cone loss remained the same.

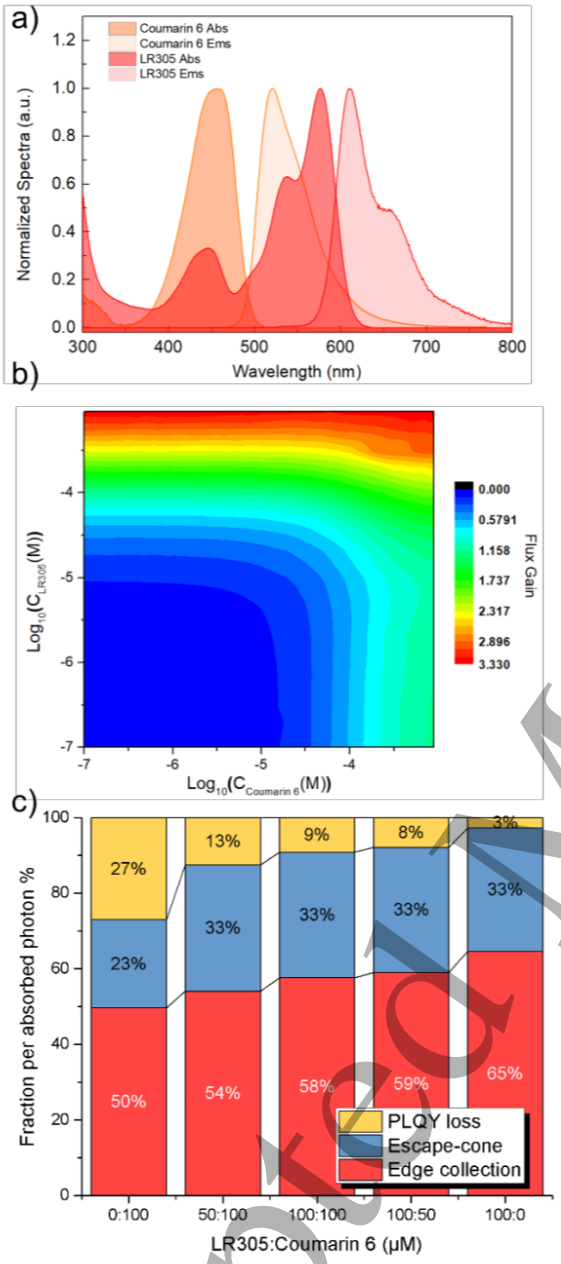

Figure 4 a) the absorption and emission spectra of Coumarin 6 and LR305, and b) heatmap of the dual-dye system showing the maximum light concentration (flux gain) obtained as a function of the concentration of LR305 and Coumarin 6 with the PLQY fixed at 0.98 and 0.78 respectively, and c) the distribution of the fate of absorbed photons at different dye ratios.

The absorbance of the waveguide substrate has been neglected in most reported simulations. However, the absorbance of the waveguide substrates can be significant, affecting the performance of the LSCs, particularly for large G.[19] To explore the importance of matrix absorption, a simulated waveguide substrate of constant absorbance (A) was added as a second absorber (concentration 10 M, thickness 0.1 cm, $\varepsilon(\lambda)$=A at all wavelengths and PLQY=0). The simulated flux gain was plotted as a function of the

geometric gain (Figure 5). It is evident that the simulated flux gain (under AM1.5g) begins to plateau as G increases. The increase in G reflects an increase in LSC size. Effectively, as the LSC becomes larger, less light reaches the edges. This is because the longer the pathlength, the more light is absorbed by the host matrix.

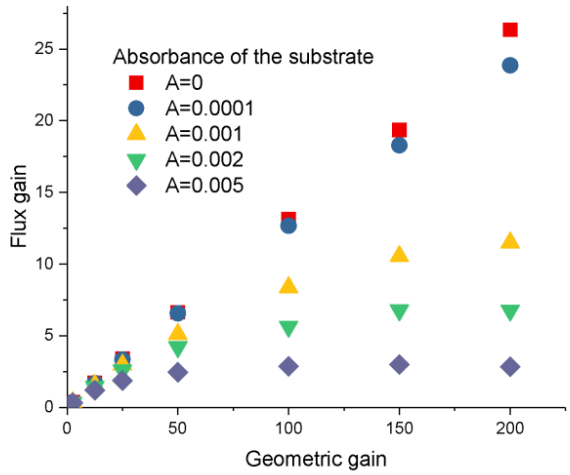

Figure 5 The simulated flux gain of LSCs in waveguide substrates with varying waveguide absorbance against the geometric gain. LR305 (0.0001 mM) was used as the fluorophore embedded in a waveguide (0.1 cm thickness, $n_{substrate}$=1.5) in the simulation. The PLQY of the substrate was set to 0.

The choice of the host material and processing methods will affect the dye distribution in LSCs. In general, there are two types of LSCs depending on the dye distribution, i.e. the thin-film LSC and the bulk-doped LSC respectively (see Figure 1b), and both can be simulated using the MCRTS-GUI. For thin-film LSCs, the effect that a different n for each layer has on the overall waveguiding efficiency is explored (Figure 6a). Changing the n of the dye-layer is shown to have a greater influence than changing the n of the clear substrate.

The bulk-doped LSC and thin-film LSC might be expected to exhibit similar behaviour for a given n of the substrate materials. As shown in Figure 6a, the simulated EQE (for single wavelength, λ = 537 nm) of a bulk-doped LSC and thin-film LSC were identical for the same n of 1.5. The n of the dye-layer and the clear substrate layer can be specified individually by the user. Here we provide two cases where the n of the dye-layer and clear substrate layer are varied. For a thin-film LSC on a clear substrate with n=1.5, the EQE increased against the n of the dye-layer, in a similar manner to the bulk-doped LSC. On the other hand, the EQE of the thin-film LSC remained almost the same regardless of changes in the n of the clear substrate, if the dye-layer is fixed at n = 1.5 (Figure 6a). Since the simulations shared the same fluorophore information and same geometry of the waveguide, η_{trapping} was the main influence on the EQE with the variation in n of the waveguide. The comparison between these two sets of simulations of the thin-film LSC show that $\eta_{trapping}$ was only dependent on the n of the dye-layer and not the clear substrate.

To further clarify the influence of the n of both the dye-layer and the clear substrate in thin-film LSCs, a series of ray tracing figures were plotted based on the simulation of a 3-layer LSC where a dye-layer is sandwiched between two clear substrate layers (Figure 6b). The n of the clear substrates was kept at 1.5

in all three waveguides while the n of the dye-layer was varied. For these examples the LSC was excited at the central position (Diagnostic Mode "on"). When the n of the dye-layer was 1.0, the emitted light was not trapped by the clear substrate layer and the photon exited the LSC through the escape cone. When the n of the dye-layer increased to 1.5, photons travelled through the dye-substrate interface with minimal reflectance. However, when the n of the dye-layer was increased to 2.0, the light was mainly constrained in the dye-layer. The observations from the three simulations indicates that η_{escape} is only related to the n of the dye-layer but not the clear substrate, consistent with the result in Figure 7a.

However, Figure 6b also shows that the n of the clear substrate can still influence the ray trace distribution in the waveguide. When the re-absorption rate was different in the dye-layer and the clear substrate-layers, the OQE and EQE of the LSC may be influenced by the ray trace distribution in the waveguide. For instance, when the re-absorption in the dye-layer was much higher than the clear substrate, a higher n of the clear substrate can help to reduce the light path in the dye-layer, leading to a reduced contribution by re-absorption. On the other hand, when the re-absorption rate in the clear substrate is greater, the n of the dye-layer can be made higher and this helps trap more rays.

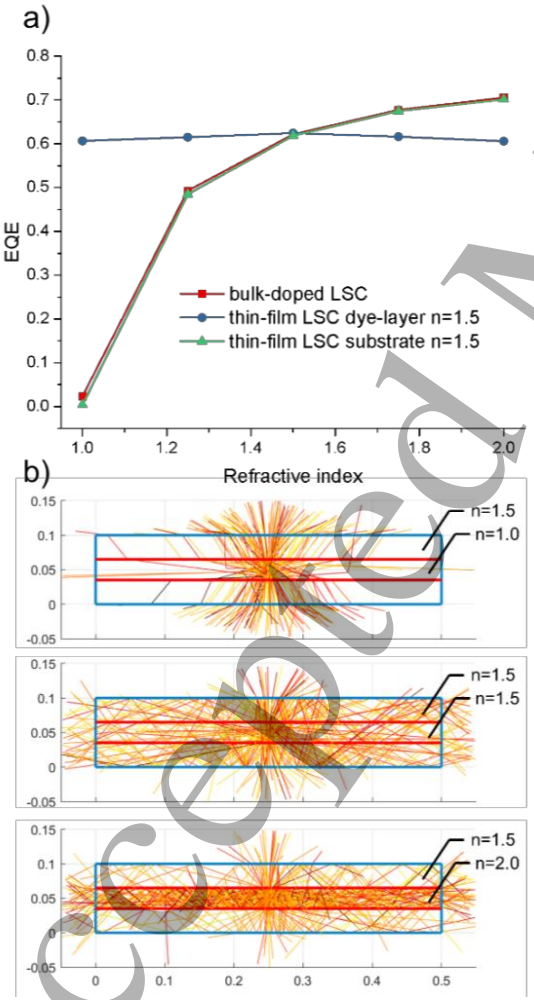

Figure 6 a) comparison of EQE versus the n of the substrate for the bulk-LSC and thin-film LSC. One thin-film LSC with the n of the dye-layer held at 1.5, while the other fixes the n of the clear substrate at

1.5. b) the simulation of a glass-dye-glass structured waveguide (Diagnostic Mode "on"). The n of both the glass layers are 1.5, while the n of the dye-layer was set to 1.0, 1.5 and 2.0 respectively.

In conclusion, we have developed the MCRTS-GUI as a user-friendly program for simulating and analyzing the performance of single-junction LSCs. The code of the MCRTS-GUI is freely available to download and can be run using MATLAB. The validation simulations described herein indicate the MCRTS-GUI can accurately simulate the basic functions of a single-junction LSC device. Three simulation examples are provided that demonstrate the functions available for MCRTS-GUI, including the use of two-dye systems and the option of adding clear substrate layers. It was also found that 'matrix absorption' although small should not be neglected when simulating LSCs, as the absorbance of the waveguide has a significant influence on the performance. We believe the MCRTS-GUI will assist both academic and commercial researchers in the design and evaluation of LSCs. In future versions of the MCRTS-GUI, we plan to include additional features, such as tandem structures with an air gap inserted or anisotropically emitting dye molecules.

Acknowledgements

This research was supported by the ARC Centre of Excellence in Exciton Science (CE170100026). This work was also made possible by support from the Australian Renewable Energy Agency which funds the project grants within the Australian Centre for Advanced Photovoltaics (ACAP). Responsibility for the views, information, or advice expressed herein is not accepted by the Australian Government. The authors acknowledge Mr. Christopher Haines for developing an early version of the Monte Carlo simulation code.

ORCID

Wallace W. H. Wong: 0000-0001-7131-8532

Kenneth P. Ghiggino: 0000-0001-6621-4448

Bolong Zhang: 0000-0002-2955-8409

Paul Mulvaney: 0000-0002-8007-3247

Notes

The authors declare no competing financial interest.

Supplementary Information

Instructions for downloading the MCRTS-GUI and the raw spectra data files used for the simulations in the paper.

References:

1. Van Sark, W. G.; Barnham, K. W.; Slooff, L. H.; Chatten, A. J.; Büchtemann, A.; Meyer, A.; McCormack, S. J.; Koole, R.; Farrell, D. J.; Bose, R., Luminescent Solar Concentrators-a Review of Recent Results. *Opt. Express* **2008,** *16* (26), 21773-21792.
2. Debije, M. G.; Verbunt, P. P. C., Thirty Years of Luminescent Solar Concentrator Research: Solar Energy for the Built Environment. *Adv. Energy Mater.* **2012,** *2* (1), 12-35.
3. McKenna, B.; Evans, R. C., Towards Efficient Spectral Converters through Materials Design for Luminescent Solar Devices. *Adv. Mater.* **2017,** *29* (28), 1606491.
4. Banal, J. L.; Zhang, B.; Jones, D. J.; Ghiggino, K. P.; Wong, W. W., Emissive Molecular Aggregates and Energy Migration in Luminescent Solar Concentrators. *Acc. Chem. Res* **2017,** *50* (1), 49-57.
5. Tummeltshammer, C.; Taylor, A.; Kenyon, A. J.; Papakonstantinou, I., Losses in Luminescent Solar Concentrators Unveiled. *Sol. Energy Mater. Sol. Cells* **2016,** *144*, 40-47.
6. van Sark, W., Luminescent Solar Concentrators – a Low Cost Photovoltaics Alternative. *Renew. Energy* **2013,** *49*, 207-210.
7. Würth, C.; Grabolle, M.; Pauli, J.; Spieles, M.; Resch-Genger, U., Relative and Absolute Determination of Fluorescence Quantum Yields of Transparent Samples. *Nature Protocols* **2013,** *8* (8).
8. Chatten, A.; Farrel, D.; Jermyn, C.; Thomas, P.; Buxton, B.; Buchtemann, A.; Danz, R.; Barnham, K. In *Thermodynamic Modelling of Luminescent Solar Concentrators*, Conference Record of the Thirty-first IEEE Photovoltaic Specialists Conference, 2005., IEEE: 2005; pp 82-85.
9. Carrascosa, M.; Unamuno, S.; Agullo-Lopez, F., Monte Carlo Simulation of the Performance of Pmma Luminescent Solar Collectors. *Appl. Opt.* **1983,** *22* (20), 3236-3241.
10. Haines, C.; Chen, M.; Ghiggino, K. P., The Effect of Perylene Diimide Aggregation on the Light Collection Efficiency of Luminescent Concentrators. *Sol. Energy Mater. Sol. Cells* **2012,** *105*, 287-292.
11. Kostro, A.; Huriet, B.; Schüler, A. In *Photonsim: Developing and Testing a Monte-Carlo Ray-Tracing Software for the Simulation of Planar Luminescent Solar Concentrators*, Proceedings of the CISBAT 2007 International Conference, Lausanne, Switzerland, 2007; pp 4-5.
12. Plachetka, T. In *Pov Ray: Persistence of Vision Parallel Raytracer*, Proc. of Spring Conf. on Computer Graphics, Budmerice, Slovakia, 1998.
13. Mulder, C. L.; Reusswig, P. D.; Velázquez, A. M.; Kim, H.; Rotschild, C.; Baldo, M. A., Dye Alignment in Luminescent Solar Concentrators: I. Vertical Alignment for Improved Waveguide Coupling. *Opt. Express* **2010,** *18* (9), 90.
14. Zhang, B.; Gao, C.; Soleimaninejad, H.; White, J. M.; Smith, T. A.; Jones, D. J.; Ghiggino, K. P.; Wong, W. W. H., Highly Efficient Luminescent Solar Concentrators by Selective Alignment of Donor–Emitter Fluorophores. *Chem. Mater.* **2019,** *31* (8), 3001-3008.
15. Zhang, B.; Soleimaninejad, H.; Jones, D. J.; White, J. M.; Ghiggino, K. P.; Smith, T. A.; Wong, W. W. H., Highly Fluorescent Molecularly Insulated Perylene Diimides: Effect of Concentration on Photophysical Properties. *Chem. Mater.* **2017,** *29* (19), 8395-8403.
16. Kaniyoor, A.; McKenna, B.; Comby, S.; Evans, R. C., Design and Response of High-Efficiency, Planar, Doped Luminescent Solar Concentrators Using Organic–Inorganic Di-Ureasil Waveguides. *Adv. Opt. Mater.* **2016,** *4* (3), 444-456.
17. Swinehart, D. F., The Beer-Lambert Law. *J. Chem. Educ.* **1962,** *39* (7), 333.
18. Shirley, J. W., An Early Experimental Determination of Snell's Law. *Am. J. Phys.* **1951,** *19* (9), 507-508.
19. Zhang, B.; Zhao, P.; Wilson, L. J.; Subbiah, J.; Yang, H.; Mulvaney, P.; Jones, D. J.; Ghiggino, K. P.; Wong, W. W. H., High-Performance Large-Area Luminescence Solar Concentrator Incorporating a Donor–Emitter Fluorophore System. *ACS Energy Lett.* **2019,** *4* (8), 1839-1844.